

To be submitted to  
Nuovo Cimento

ISTITUTO NAZIONALE DI FISICA NUCLEARE  
Laboratori Nazionali di Frascati

LNF-84/49(P)  
16 Luglio 1984

G.P.Capitani, E.De Sanctis, P.Levi-Sandri, M.Bernheim, S.Turck-Chièze,  
S.Frullani and J.Mougey: MONTE-CARLO STUDY OF PROTON  
MULTIPLE SCATTERING IN (e,e'p) REACTIONS

MONTE-CARLO STUDY OF PROTON MULTIPLE SCATTERING IN  $(e, e'p)$  REACTIONS

G.P.Capitani, E.De Sanctis, P.Levi-Sandri  
INFN - Laboratori Nazionali di Frascati

M.Bernheim, S.Turck-Chièze  
Département de Physique Nucléaire à Haute Energie, CEN Saclay, Gif-sur-Yvette (France)

S.Frullani  
Istituto Superiore di Sanità, Laboratorio di Fisica, Roma, and INFN - Sezione Sanità, Roma

J.Mougey  
DRF/CPN, Centre d'Etudes Nucléaires, Grenoble (France)

**ABSTRACT**

Distortion effects on the spectral function extracted from  $(e, e'p)$  experiments, because of the multiple scattering of the proton with the residual nucleus, have been evaluated by means of a Monte-Carlo code. The calculation was carried out for the  $^{16}\text{O}(e, e'p)^{15}\text{N}$  reaction, under the kinematical conditions of an experiment performed in Saclay.

The results obtained indicate that about 50% of the knock-out protons undergo a second scattering. The missing energy spectrum is largely distorted, while the momentum distributions are slightly modified. The Koltun's sum rule is better satisfied taking into account the multiple scattering contributions.

## 1 — INTRODUCTION

One of the open problems in the study of quasi free  $(e, e'p)$  reactions concerns the final state interactions between the outgoing proton and the residual nucleus. These interactions are usually taken into account by distorting the outgoing proton's wave function by means of an optical nuclear potential. Protons which have interacted with the imaginary part of the potential are considered lost from the reaction channel under consideration. On the other hand, a proton coming from another channel and whose momentum is changed during the interaction with the residual nucleus, may reach the detector. These protons, if misinterpreted as produced by a pure quasi-free reaction, give rise to false values of missing energy and recoil momenta.

In this paper we report the results of a calculation performed by means of a Monte-Carlo code ("MULDIF"), which completely simulates an  $(e, e'p)$  reaction in a given nucleus, taking into account multiple coulomb and nuclear scattering effects which the outgoing proton undergoes in crossing through the residual nucleus. Sections 2 and 3 deal with the general features of the  $(e, e'p)$  reaction and the Koltun energy-weighted sum rule <sup>(1)</sup>. Section 4 describes the general flow of the calculations and discuss the Monte-Carlo sampling techniques. Section 5 reports on the results of a calculation carried out for the  $^{16}\text{O}(e, e'p)^{15}\text{N}$  process. In section 6 the results obtained are used to correct the proton's missing energy spectrum and the energy weighted Koltun's sum rule.

## 2 — GENERAL FEATURES OF THE $(e, e'p)$ REACTION

In the oversimplified Plane Wave Impulse Approximation (PWIA) picture of the  $A(e, e'p)B$  reaction the two sides of the reaction diagram are completely separated (Fig. 1 (a)); then the cross-section can be written as:

$$\frac{d^6\sigma}{dE'_0 d\Omega'_0 dE'_1 d\Omega'_1} = K |M_{ep}|^2 S(E, \mathbf{p}_1) \quad , \quad (1)$$

where  $K$  is a kinematical factor,  $|M_{ep}|^2$  is, apart from kinematical and off the mass shell corrections,

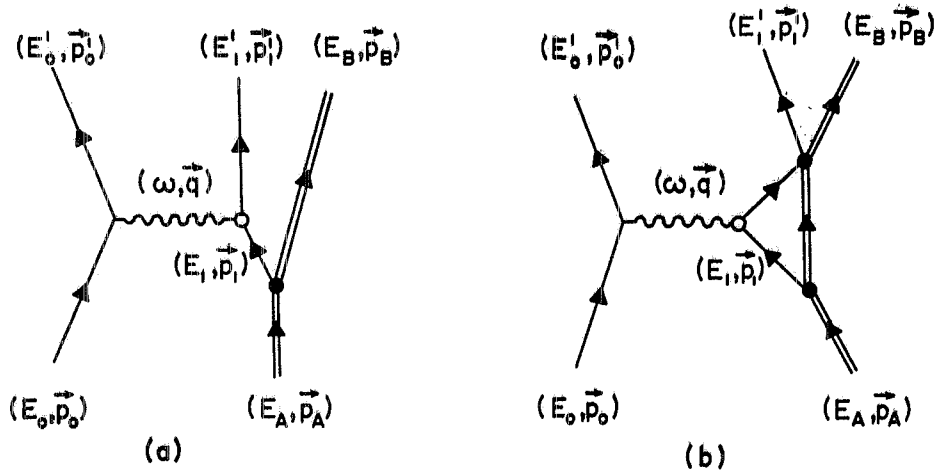


Fig. 1 - One-photon-exchange diagram for the  $A(e, e'p)B$  reaction in PWIA (a) and in DWIA (b).

the elastic electron-proton scattering amplitude, and  $S(E, \vec{p}_1)$  is the so-called spectral function of the initial nucleus. This function represents the compound probability of finding in the initial nucleus  $A$  a proton with momentum  $\vec{p}$  and separation energy  $E_S = E + T_B$ ;  $E$  is the missing energy of the reaction:  $E = M + (E_B^2 - p_B^2)^{1/2} - M_A$ ,  $M$  and  $M_A$  are the proton's and the initial nucleus' rest masses,  $E_B$  and  $T_B$  are the residual nucleus' total and kinetic energies, and  $\vec{p}_B$  the relevant momentum.

The most serious complications to this oversimplified description come from the proton-nucleus interaction (Fig. 1 (b)), which destroys the simple relation between the recoil momentum and the initial nucleon momentum and the factorization of the cross-section.

It is conceptually useful to split the interaction between the proton and the residual nucleus  $B$  into two different types:

- (a) the "elastic channel", where the proton undergoes small angles, essentially elastic scattering. The flux of particles in this channel is greatly reduced as compared to *PWIA* results; typically by a factor  $\approx 3$ , for protons of 100-200 *MeV* energies and  $A \approx 40$ . To correct the data for this distortion, the best that presently can be done amounts to Distorted Wave Impulse Approximation (*DWIA*) calculations. Here, the plane wave is replaced by a distorted wave calculated in a complex optical potential as determined from  $(p - B)$  elastic scattering data. Hereby one assumes that the optical potential is independent of whether the  $B$  nucleus is highly excited or in its ground state, an approximation that still need to be tested <sup>(2)</sup>.

(b) the "inelastic channel" in which 70% of the flux goes: the proton "disappears" by losing enough energy not to get out of the nucleus or it "reappears" at much lower energy. For this process we are presently lacking a quantitative description. In general, this reaction channel, which receives much of the flux that disappears through the imaginary part of the optical potential, is hoped to lead to a smooth and small background in the quasi-free scattering region. Indeed, due to very large phase-space available, this strength can be expected to spread out over an energy and momentum region much larger than the quasi-free one. Considering that this channel contains the dominant part of the flux, such "catastrophic" interactions do pose a major problem, particularly if one is interested in deep-hole states or in the application of energy-weighted sum rules.

In the usual *DWIA* treatment, it is assumed that the distorting potential does not change the outgoing momenta too much, so that the cross-section keeps a factorized form:

$$\frac{d^6\sigma}{dE'_0 d\Omega'_0 dE'_1 d\Omega'_1} = K |M_{ep}|^2 S^D(E, \mathbf{p}'_1, \mathbf{p}_B) \quad . \quad (2)$$

The "distorted" spectral function  $S^D$  depends upon both  $\mathbf{p}'_1$  and  $\mathbf{p}_B$ . It has been shown by Boffi and collaborators <sup>(3)</sup> that the validity of this factorized *DWIA* expression is restricted to particular kinematical conditions.

### 3 — KOLTUN ENERGY-WEIGHTED SUM RULE

Having (hopefully) measured the entire  $(E, \mathbf{p}_1)$  region where the spectral function differs significantly from zero, one can apply the Koltun's <sup>(1)</sup> energy-weighted sum rule. It relates the total binding energy per nucleon  $E_A/A$ , known from nuclear masses, to the average missing and kinetic energies  $\langle E \rangle$  and  $\langle T \rangle$  of all nucleons:

$$\frac{E_A}{A} = \frac{1}{2} \left( \frac{M_B - M}{M_B} \langle T \rangle - \langle E \rangle \right) \quad , \quad (3)$$

where  $M_B$  is the residual nucleus rest mass.

For the case of  $(e, e'p)$  experiments, since only protons are removed, equation (3) needs to be

modified as follows:

$$\frac{E_Z}{Z} = \frac{1}{2} \left( \frac{M_B - M}{M_B} \frac{1}{n} \int \frac{p_1^2}{2M} S(E, \mathbf{p}_1) dE d\mathbf{p}_1 - \frac{1}{n} \int E S(E, \mathbf{p}_1) dE d\mathbf{p}_1 \right), \quad (3')$$

where  $n = \int S(E, \mathbf{p}_1) dE d\mathbf{p}_1$ . That is  $E_A/A$  has to be corrected for the coulomb and symmetry energies, and  $\langle T \rangle$  and  $\langle E \rangle$  are expressed in term of the undistorted spectral function.

In Table 1 we report the values obtained for  $\langle T \rangle$ ,  $\langle E \rangle$  and  $\Delta$ , the difference between the two sides of equation (3'), using experimental data from Saclay (4,5). One sees that, with the exception of  $^{40}\text{Ca}$ , the sum rule is by far not fulfilled:  $\Delta$  is significantly different from zero and always negative. It has been checked this result is almost free of the ambiguities coming from the analysis of the data (absolute value uncertainty, difficulties in disentangling the different shells ambiguities in the *DWIA* treatment). By evaluating the sum rule directly from the uncorrected measured spectral function (*PWIA* treatment) deviation values  $\Delta_{nc}$  were obtained, nearly equal to  $\Delta$  ones, showing that the discrepancy is not likely to be attributed to uncertainties in the distortion correction.

**TABLE 1** - Deviation  $\Delta$  from the Koltun's sum rule observed when considering the proton mean kinetic ( $T$ ) and removal ( $E$ ) energies from (e,e'p) experiments on given nuclei.  $E_Z/Z$  is the total binding energy per proton.  $\Delta_{nc}$  are the deviations calculated without distortion corrections on the experimental spectral function (*PWIA*).  $E_{max}/p_{max}$  gives the energy/momentum range upper boundary (the lower one being 0 MeV and 0 MeV/c) over which the mean energies have been determined.

Nucleus	$E_{max}/p_{max}$ (MeV/MeV/c)	$E_Z/Z$ (MeV)	$\langle E \rangle$ (MeV)	$\langle T \rangle$ (MeV)	$\Delta$ (MeV)	$\Delta_{nc}$ (MeV)	Ref.
$^9\text{Be}$	60/300	-8.90	29.1	16.0	$-1.4 \pm 0.5$	-1.7	(5)
$^{12}\text{C}$	60/280	-6.93	23.4	16.9	$-2.9 \pm 0.7$	-2.5	(4)
$^{16}\text{O}$	60/300	-7.09	25.2	14.4	$-1.7 \pm 0.5$	-1.3	(5)
$^{28}\text{Si}$	60/250	-7.02	24.0	17.0	$-3.1 \pm 0.6$	-3.3	(4)
$^{40}\text{Ca}$	70/250*	-6.73	27.8	16.6	$-0.9 \pm 0.5$	-1.1	(4)
$^{58}\text{Ni}$	70/240*	-7.11	25.0	18.8	$-3.6 \pm 0.7$	-3.6	(4)

As the derivation of the sum rule (eq.(3')) has been made under the assumption of the absence of 3- or more-body forces in the hamiltonian, some authors (6,7,8) have attributed the non-zero and negative value of  $\Delta$  to the existence of repulsive 3-body forces contribution.

However, the breakdown of the sum rule may have a much more trivial explanation, that is the limited energy/momentum range used to determine  $\langle E \rangle$  and  $\langle T \rangle$  from experiment. In fact, the application of the sum rule to the  $^{16}\text{O}(e, e'p)$  data <sup>(5)</sup> over a wider energy range ( $0 < E < 100 \text{ MeV}$  instead of  $0 < E < 60 \text{ MeV}$ ), shows that 12% of the measured strength is in the region between 60 and 100 MeV. This region, if interpreted as a part of the spectral function contributes for 3.25 MeV to the sum rules, which makes it overfilled ( $\Delta = +1.93$ ), as shown in Table 2. Obviously it must be estimated how much of the strength located in this region may come from the multiple collisions background, which has to be subtracted. In the absence of a reliable calculation of this background it is difficult to draw any definite conclusion on this matter. In fact the "standard" distortion correction is not at all adequate, because - as we remarked - some of the protons removed from the spectral function, via the imaginary part of the optical potential, can still give their contribution with a "wrong" binding energy and recoil momentum.

TABLE 2 - Results for the energy sum rule for  $^{16}\text{O}$ . Symbols have the same meaning as in Table 1.

Separation energy range	Fraction of strength	$\langle T \rangle$	$\langle E \rangle$	$\Delta$	$\Delta_{nc}$
0/60	88	14.4	25.2	-1.70	(-1.30)
0/100	100	14.3	31.4	1.93	

#### 4 — DESCRIPTION OF THE PROGRAM

The program "MULDIF" is a FORTRAN 77 code which completely simulates an  $(e, e'p)$  reaction in a given nucleus, taking into account the interactions which the scattered proton undergoes in crossing the residual nucleus. Here we describe the general flow of the calculation and discuss the Monte-Carlo sampling techniques.

The goal of the calculation is to produce a distorted spectral function as output from an undistorted one given as input. The main features of the program are the following:

- (i) spectral functions for protons and neutrons were assumed to be identical. The missing energy dependence was chosen as to reproduce the position of the peaks in the experimental distributions. The shape of the peaks was fitted with a superposition of Lorentz curves <sup>(9)</sup>. The behaviour of momentum distributions was fitted with gaussian curves whose central values and widths agree with the experimental values of the different shells. This spectral function fulfills the sum rules;
- (ii) the energy of the incident electron was kept equal to the value used in the experiment <sup>(5)</sup> we were interested in correcting the data;
- (iii) the nucleon partner of the reaction (whether a proton or a neutron) was chosen according to the relative  $\sigma_{ep}$  and  $\sigma_{en}$  total cross-sections. The formulae used were those given by Mougey <sup>(10)</sup> for the free  $\sigma_{eN}$  cross-section in which the electric and magnetic form factors are those given by Janssens et al. <sup>(11)</sup> for a free nucleon.
- (iv) the physical point where the  $(e, e'N)$  reaction takes place was sampled according to the nuclear proton density. Also the separation energy and the momentum modulus of the initial nucleon were sampled according to the spectral function. The initial direction of motion for the nucleon was uniformly extracted in the  $4\pi$  solid angle;
- (v) the angles of the scattered electron were extracted, inside the experimental acceptance, according to the free  $(e, N)$  cross-section;
- (vi) the occurrence of a nuclear scattering was sampled according to the mean free path  $\lambda$  for a nucleon in nuclear matter:

$$\lambda^{-1} = \sigma_p \rho_p + \sigma_n \rho_n \quad ,$$

where  $\sigma_p$  and  $\sigma_n$  are the total  $(p-p)$  and  $(p-n)$  cross-sections at relevant energies and  $\rho_p$  and  $\rho_n$  are the proton and neutron densities. Pion production was ignored. The coulomb contribution to the  $(p-p)$  cross section was neglected and  $(n-n)$  cross-section and angular distribution were taken equal to the  $(p-p)$  ones. The occurrence of further nuclear scatterings was neglected;

- (vii) once the reaction point was determined, a choice was made to whether the partner of the second scattering was a proton or a neutron, following a procedure similar to that of step (iii). By analogy, the separation energy and the momentum modulus of the second nucleon before the scattering process were sampled according to the spectral function at that time;



(viii) the directions of the two nucleons, providing there was a nuclear scattering, were sampled according to the angular dependence of the free elastic process. The differential cross-section for the  $(p - p)$  scattering was assumed to be isotropic in the center-of-mass system for proton energies up to 500 MeV. The  $(p - n)$  process was represented by the following semiempirical fits to the Hess data <sup>(13)</sup>:

$$\left(\frac{d\sigma}{d\Omega}\right)_{(n-p)} = A_0 + A_3\mu^3, \quad (0 < \mu < 1, \quad 0 < E < 500 \text{ MeV})$$

$$\left(\frac{d\sigma}{d\Omega}\right)_{(n-p)} = A_0 + A_4\mu^4, \quad (-1 < \mu < 0, \quad 0 < E < 300 \text{ MeV})$$

$$\left(\frac{d\sigma}{d\Omega}\right)_{(n-p)} = A_0 + A_6\mu^6, \quad (-1 < \mu < 0, \quad 300 < E < 500 \text{ MeV})$$

where  $E$  is the incident nucleon energy and  $\mu$  is the cosine of the scattering angle in the center-of-mass system. The values of  $A_3$ ,  $A_4$  and  $A_6$  are given at relevant energies in Table 3;

TABLE 3 - Parameters of the angular distribution of (p-n) scattering in the center-of-mass system (see text for the meaning of symbols).

Incident particle Laboratory Energy (MeV)	(n - p) $A_0$	Parameters		$(mb/sr)$ $A_6$
		$A_3$	$A_4$	
0	1592.0	0	0	0
40	12.0	7.0	7.0	0
80	5.2	8.1	8.3	0
120	3.3	6.6	9.0	0
160	2.3	3.9	7.7	0
200	2.0	3.6	6.5	0
240	1.9	3.6	6.2	0
280	1.8	3.6	6.0	0
320	1.7	3.6	0	7.8
360	1.5	3.6	0	7.4
400	1.4	3.6	0	7.0
440	1.3	3.6	0	6.7
480	1.2	3.6	0	6.4
520	1.1	3.6	0	6.1

- (ix) at steps (iv) and (vi) an uniform density distribution was assumed;
- (x) inside the nucleus, nucleons were treated as free on-shell particles;
- (xi) the kinetic energy of the nucleon outside the nucleus was assumed to be smaller than inside by the amount of the separation energy determined at steps (iv), (vi), and (vii), and the momentum of the proton outside the nucleus was adjusted accordingly;
- (xii) for each proton ejected from the nucleus apparent values of separation energy and recoil momentum were calculated.

## 5 — RESULTS FROM MULDIFF

The calculation was carried out for the  $^{16}\text{O}(e, e'p)^{15}\text{N}$  process. The VAX 11/780 of the Frascati Laboratory was used; a total CPU time of about 34 hours was needed to examine 3 482 400 events.

In Fig. 2 we show the distorted missing energy spectra resulting from calculations having as input a spectral function whose energy spectrum consists of a single channel, centered at a given  $E$  value. As shown, only  $\approx 50\%$  of the knock-out protons keep the original missing energy. Final state interactions shift almost all remaining protons toward higher  $E$  values, only  $\approx 1.5\%$  being displaced to lower energies. This result was found to be independent of the original missing energy value and of the shape of the momentum distribution.

In Fig. 3 and Fig. 4 we show the results of the calculation for the missing energy spectrum and for the momentum distributions, respectively. Solid (dashed) curves refer to the spectral function with (without) final state interactions, the hatched histogram to the "background" due to nuclear scattering. In Fig. 4 the energy regions of Fig. 4 (a), 4 (b) and 4 (c) correspond to  $1p_{1/2}$  (a),  $1p_{3/2}$  (b,c) hole states, respectively. The main contribution in Fig. 4 (d) comes from the  $1s_{1/2}$  hole state.

The input spectral function was chosen according to point (i) of the previous Section. Each ejected nucleon was examined, free from detection, and stored into missing energy and initial momentum bins. It was found that 49.4% of the knock-out nucleons underwent a second nuclear scattering, while the effect of coulomb scattering resulted to be negligible.

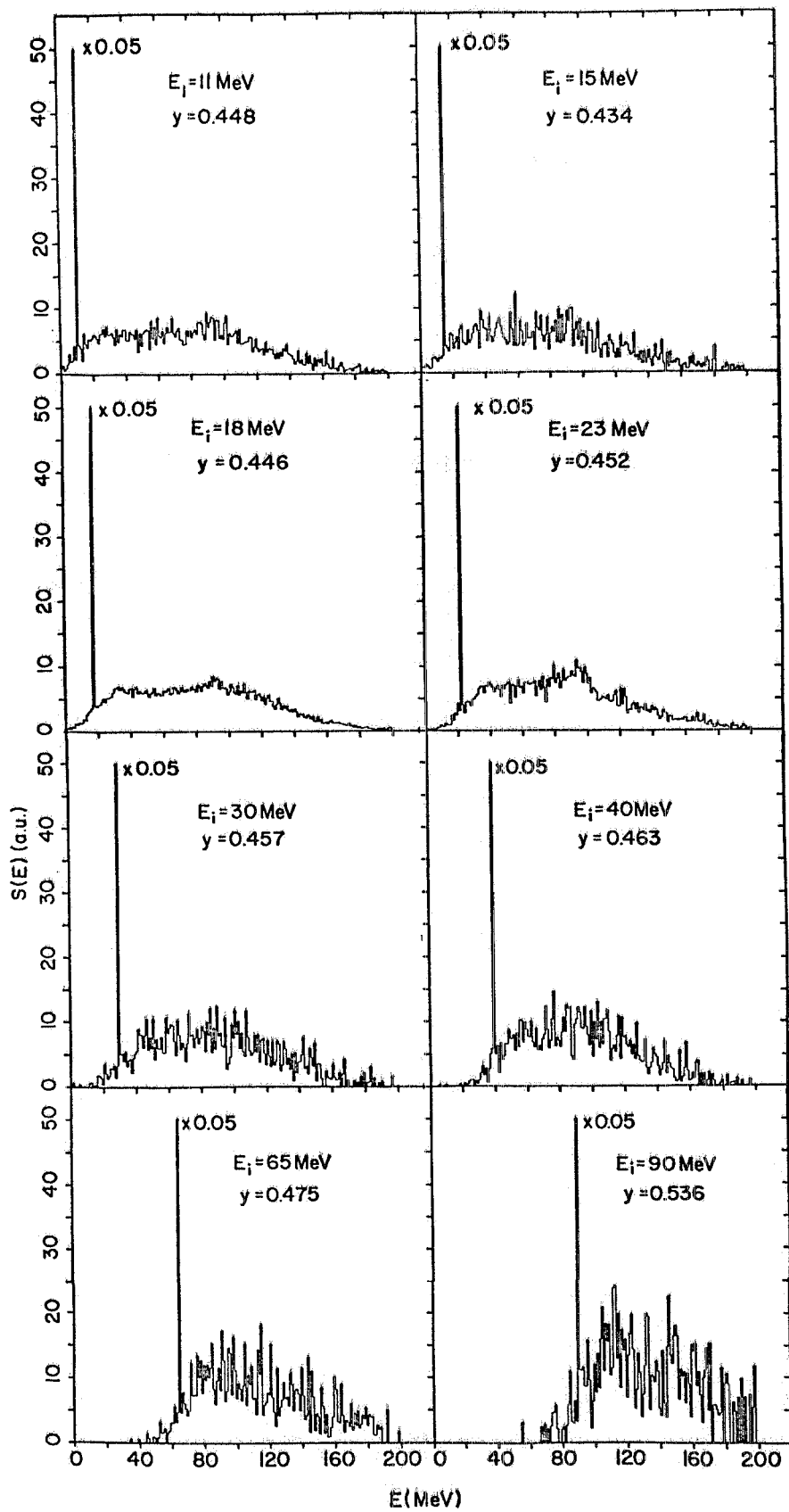


FIG. 2 - Calculated missing energy spectra including final state interactions. The input spectral functions were a single occupied channel centered at the given  $E$  values;  $y$  is the fraction of events shifted at energies different from  $E$ .

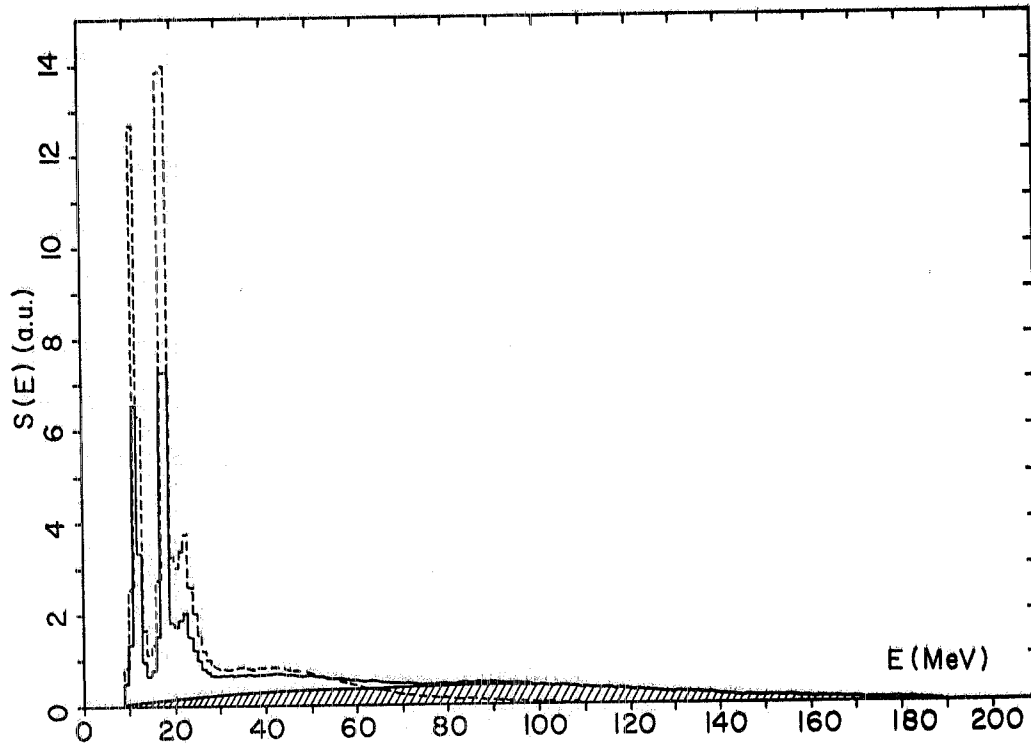


FIG. 3 - The calculated missing energy spectrum for the  $^{16}\text{O}(e,e'p)^{15}\text{N}$  reaction with (full line) and without (dashed line) final-state interactions. The hatched histogram refers to "background" due to nuclear scattering only.

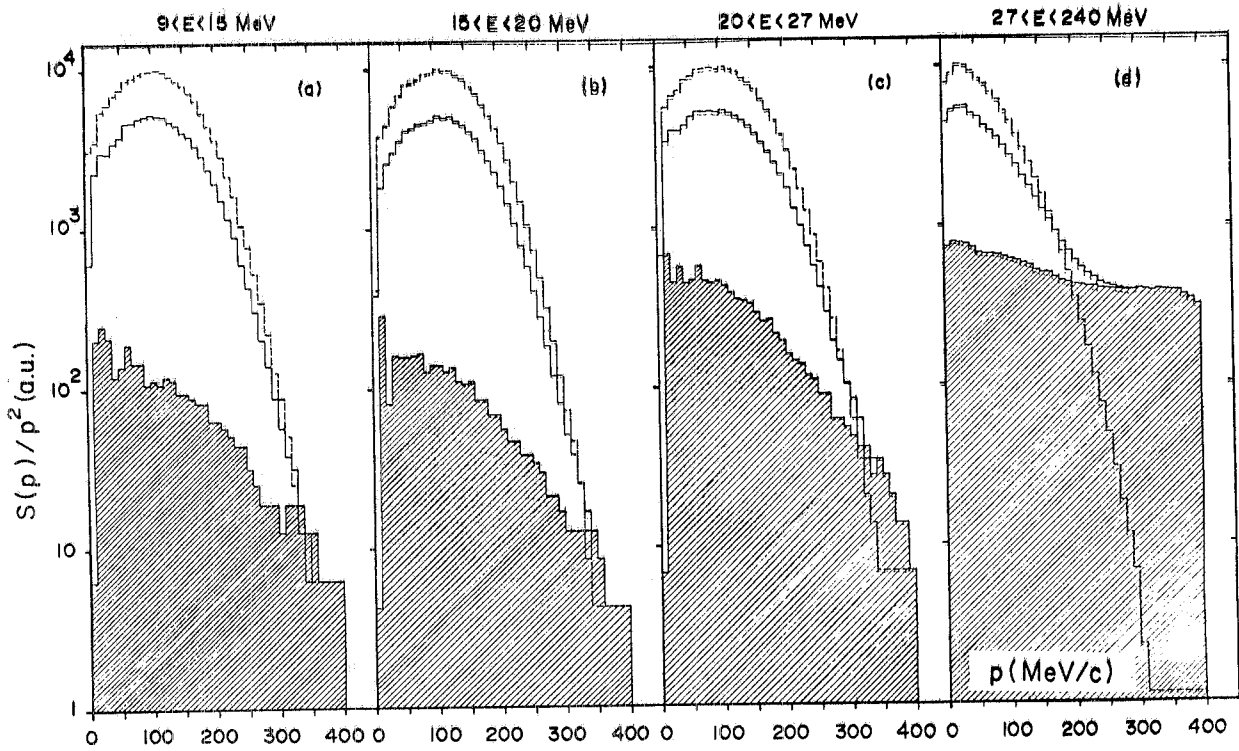


FIG. 4 - The calculated momentum distributions for the  $^{16}\text{O}(e,e'p)^{15}\text{N}$  reaction with (full line) and without (dashed line) final-state interactions. The hatched histogram refers to "background". The different energy regions correspond to  $1p_{1/2}$  (a),  $1p_{3/2}$  (b,c) hole states. The main contributions in (d) comes from the  $1s_{1/2}$  hole states.

According to the results shown in Fig. 2, the multiple scattering collision background gradually increases as  $E$  increases, reaching a maximum around 90 MeV, and then decreases. Moreover it stays the only contribution above 95 MeV. The shapes of the momentum distributions (Fig. 4), are not very much changed (except for the high  $E$  region), although final state interactions lead to a reduction of the integrated cross-section by a factor decreasing with increasing central values of corresponding missing energy regions. The percentage of second interactions for the different shells is found to be 48.2%, 48.8% and 51.3% for the  $1p_{1/2}$ ,  $1p_{3/2}$ , and  $1s_{1/2}$  states, respectively.

About 20% of the multiple collision background comes from an  $(e, e'n)$  process followed by a  $(n, p)$  scattering.

Having considered the p-shape contributions as single hole states, it is reasonable to compare the values of the absorption factors

$$\eta = \frac{\int_0^{p_{max}} S^D(E, \mathbf{p}_1) d\mathbf{p}_1}{\int_0^{\infty} S(E, \mathbf{p}_1) d\mathbf{p}_1}$$

obtained by our calculation with those derived by Boffi's <sup>(14)</sup> theoretical evaluations for different sets of bound states and optical potentials. The results are summarized in Table 4.

TABLE 4 - Absorption factor values as derived by MULDIF results and by Boffi's calculations for the given bound-states and optical potentials.

Bound-state Optical Potential	$p_{1/2}$ (10 — 15 MeV)	$p_{3/2}$ (15 — 20 MeV)	$p_{3/2}$ (20 — 25 MeV)
Elton-Swift-Glassgold-Kellog	0.66	0.71	0.69
Elton-Swift-Jackson	0.50	0.66	0.67
Gogny-Jackson	0.51	0.65	0.66
MULDIF	0.53	0.53	0.57

## 6 — APPLICATION TO ANALYSIS OF EXPERIMENTAL DATA

As described in the previous section, "MULDIF" is a program that transforms a given input spectral function in an output spectral function which is distorted for the effects of multiple

scattering. Therefore, the real problem to be faced by is the following: how can we use the results of "MULDIF" for correcting a measured spectral function?

The adopted procedure was the following. As the introduction of final state interactions distorts mainly the missing energy spectrum, we ignored the effects on momentum dependence. Moreover we neglected the case when multiple scattering shifts protons to lower missing energy values.

Having written the input missing energy spectrum  $S_I(E_i)$  in the form of an histogram:

$$S_I(E_i) = 4\pi \sum_l S(E_i, p_l) p_l^2 \Delta p_l \quad ,$$

we have calculated, for each channel  $i$ , the discrete function  $f_{ij}$  representing the fraction of  $S_I(E_i)$  that multiple interactions, according to "MULDIF" calculations, displace to the  $j$ -th channel of the distorted missing energy distribution,  $S_D(E_j)$ .

Obviously:

$$\sum_j f_{ij} = S_I(E_i) \quad .$$

Then, starting from the measured energy spectrum  $S_M(E_i)$ , we were able to deduce the "true" spectrum  $S_T(E_i)$  in the following way: the value of the first channel of  $S_T$  was obtained from the relation:

$$S_T(E_1) = \sum_{j=1}^N \frac{f_{1j}}{f_{11}} S_M(E_1) = S_M(E_1) + \sum_{j=2}^N \frac{f_{1j}}{f_{11}} S_M(E_1) \quad ,$$

where the last summation represents the part of  $S_T(E_1)$  which, because of the final state interactions, is wrongly attributed to others energy channels of the spectral function.  $N$  is the number of energy bins.

In order to calculate the content of the second channel,  $S_T(E_2)$ , it is convenient to define the function:

$$S_M^1(E_i) = S_M(E_i) - S_T(E_1) = S_M(E_i) - \frac{f_{1i}}{f_{11}} S_M(E_1) \quad .$$

Then, applying again the previous procedure to the spectral function  $S_M^1$ , we have:

$$S_T(E_2) = \sum_{j=2}^N \frac{f_{2j}}{f_{22}} S_M^1(E_2) \quad .$$

The particular form of previous equations suggests the following recurrent formulae:

$$S_T(E_n) = \sum_{j=n}^N \frac{f_{nj}}{f_{nn}} S_M^{n-1}(E_n) \quad ,$$

$$S_M^n(E_i) = S_M^{n-1}(E_i) - \frac{f_{ni}}{f_{nn}} S_M^{n-1}(E_n) \quad ,$$

$$S_M^0(E_k) = S_M(E_k) \quad .$$

Following the above procedure we deduced the undistorted missing energy spectrum from the spectrum for the  $^{16}\text{O}(e, e'p)^{15}\text{N}$  reaction measured at the Saclay ALS accelerator, using the two-spectrometers set-up of the HE1 end station <sup>(15)</sup>. The kinematics conditions are given in Table 5. It must be pointed out that the  $f_{ij}$  coefficients have been obtained by using only the 25 335 protons that entered the detector out of the 3 482 400 events computed by "MULDIF". Moreover we neglected those events having two protons in the final state, both being detected. The result is shown in Fig. 5: dashed and full lines refer to measured and undistorted missing energy spectra, respectively. As seen, the correction procedure increases the intensity of  $S(E)$  in the region  $E < 40 \text{ MeV}$  at the expense of the strength in the high missing energy region.

TABLE 5 - Kinematical conditions for the  $^{16}\text{O}(e, e'p)^{15}\text{N}$  experiment <sup>(5)</sup>.

incident electron energy : $E_0 = 500 \text{ MeV}$
scattered electron energy acceptance : $E'_0 = 280 - 400 \text{ MeV}$
electron scattering angle : $\theta_{E'_0} = 59^\circ$
electron spectrometer diaphragm : $\theta = \pm 17.0 \text{ mrad}$ ; $\phi = \pm 100.0 \text{ mrad}$
scattered proton energy acceptance : $E'_1 = 94.5 - 109.8 \text{ MeV}$
proton scattering angles : $\theta_{E'_1} = 32.5^\circ \quad 35.0^\circ \quad 38.0^\circ \quad 40.0^\circ \quad 43.0^\circ \quad 45.5^\circ \quad 48.0^\circ \quad 50.5^\circ$
$53.0^\circ \quad 55.5^\circ \quad 58.0^\circ \quad 60.8^\circ \quad 63.0^\circ \quad 65.5^\circ \quad 68.0^\circ \quad 73.0^\circ \quad 78.0^\circ \quad 80.5^\circ \quad 83.0^\circ \quad 88.0^\circ$
proton spectrometer diaphragm : $\theta = \pm 17.33 \text{ mrad}$ ; $\phi = \pm 70.0 \text{ mrad}$

We have calculated the quantities  $\langle T \rangle$ ,  $\langle E \rangle$  and  $E_Z/Z$  for the measured spectral function and for the "corrected" one. The latter was constructed by using the undistorted missing energy spectrum and the measured momentum distributions. The results are shown in Fig. 6 where, again, dashed and solid line refer, respectively to values obtained from measured and "corrected" spectral functions. As shown the "corrected"  $\langle E \rangle$  values are lower, while the  $\langle T \rangle$  ones keep quite unchanged. Consequently the  $E_Z/Z$  value shows a better agreement with the mass formula prediction, although it still does not reach saturation.

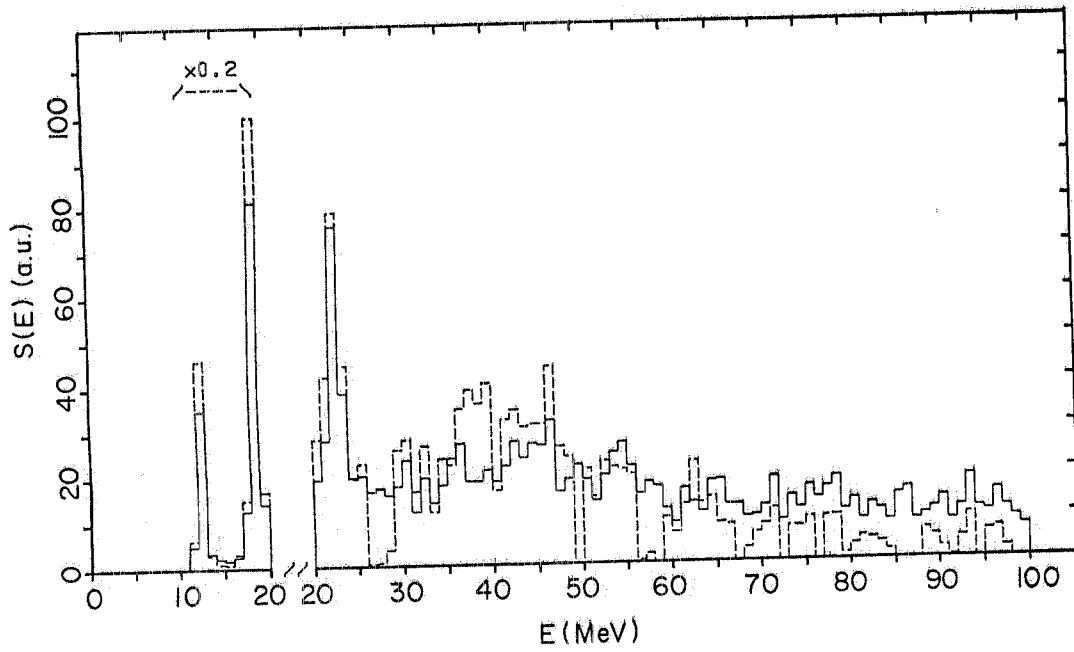


FIG. 5 - Measured (full line) and corrected (dashed line) missing energy spectra for the  $^{16}\text{O}(e,e'p)^{15}\text{N}$  reaction.

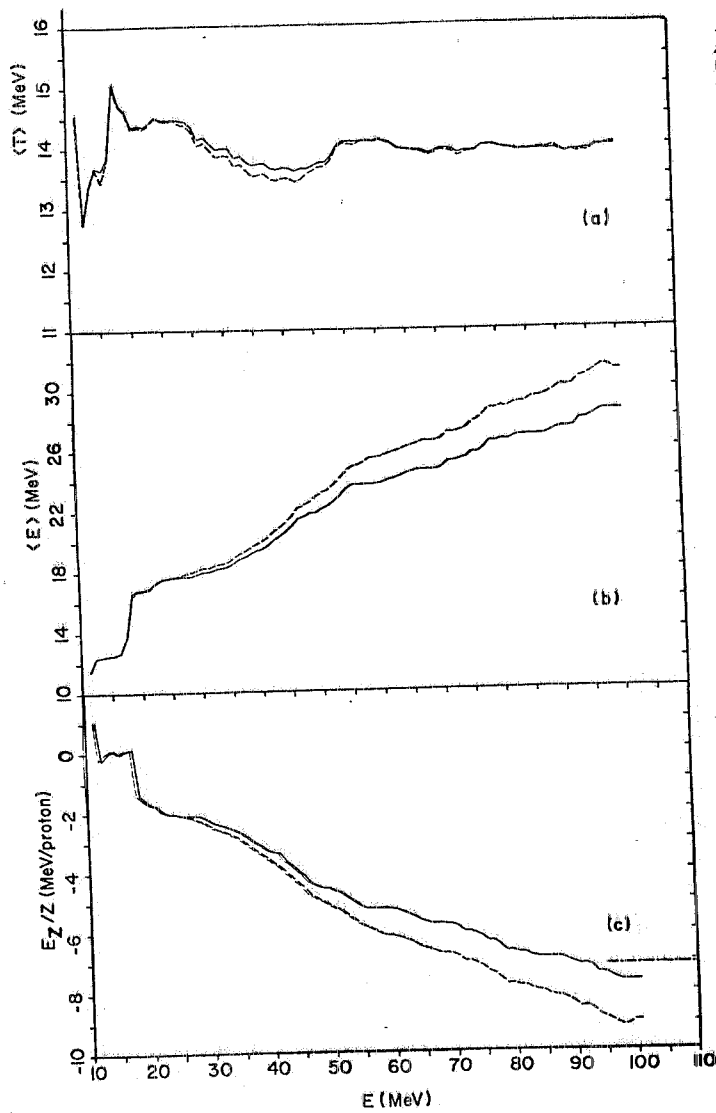


FIG. 6 - Values for  $\langle T \rangle$  (a),  $\langle E \rangle$  (b) and  $E_z/Z$  (c) obtained from measured (dashed lines) and corrected (full lines) spectral functions. The dot-dashed line in (c) is the  $E_z/Z$  value from mass formula.



## 7 — CONCLUSION

To summarize we can draw the following conclusions:

- (1) the effect of final state interactions is quite sizeable: about 50% of the knocked-out nucleons undergo a second nuclear scattering;
- (2) the final state interactions distort largely the missing energy spectrum displacing protons from low to high missing energy regions;
- (3) the shapes of the distorted momentum distributions are not very much different from the undistorted ones except for the one corresponding to the high missing energy region;
- (4) the Koltun's sum rule, although not fulfilled, is better satisfied when corrections for multiple collision are applied.

## REFERENCES

- (1) D.S. Koltun, *Phys. Rev. Lett.* 7(1982)182.
- (2) V.E. Herscovitz, *Nucl. Phys.* A161(1970)321.
- (3) S. Boffi, C. Giusti, F.D. Pacati and S. Frullani, *Nucl. Phys.* A319(1979)461.
- (4) J. Mougey et al., *Nucl. Phys.* A262(1976)461.
- (5) M. Bernheim et al., to be published.
- (6) D.W.E. Blatt and B.H.T. McKellar, *Phys. Lett.* 52B(1974)10.
- (7) S. Yang, *Phys. Rev.* C10(1974)2067
- (8) A. Faessler et al., *Phys. Rev.* C11(1975)2069.
- (9) H. Orland and L. Scheffer, *Nucl. Phys.* A299(1978)442.
- (10) J. Mougey, Thesis, Université de Paris-Sud, (1976).
- (11) T. Janssens et al., *Phys. Rev.* 142(1966)922.
- (12) H.W. Bertini, *Phys. Rev.* 131(1963)1801.
- (13) W.N. Hess, *Rev. Mod. Phys.* 30(1958)368.
- (14) S. Turk-Chièze, *Lect. Notes in Phys.* 137(1980)251 and references therein.
- (15) P. Leconte et al., *Nucl. Instr. Meth.* 169(1980)401.